TECHNICAL NOTE

www.rsc.org/loc

"Smart" mobile affinity matrix for microfluidic immunoassays

Noah Malmstadt, Allan S. Hoffman* and Patrick S. Stayton*
Department of Bioengineering, University of Washington, Seattle, WA 98195, USA

Received 27th November 2003, Accepted 12th March 2004
First published as an Advance Article on the web 6th April 2004

There is a current need for simple methods for immobilizing biomolecules within microfluidic channels. Here, a technique is reported for reversibly immobilizing immunoassay components in a channel zone that can be simply controlled by integrated heating elements. Latex beads were modified with the temperature-responsive polymer poly(*N*-isopropylacrylamide) (PNIPAAm) and co-modified with biotinylated poly(ethylene glycol) (PEG). PNIPAAm undergoes a hydrophilic-to-hydrophobic transition when the temperature is raised above the lower critical solution temperature (LCST) (~ 28 °C in the solutions used here). This reversible transition drives the aggregation and dis-aggregation of the modified beads in heated zones within poly(ethylene terephthalate) (PET) microchannels. Biotinylated monoclonal antibodies for the drug digoxin were bound *via* streptavidin to the biotin-PEG-coated beads. These antibody-functionalized beads were then reversibly immobilized by aggregation and hydrophobic adhesion to the surface of PET microfluidic channels in response to a thermal stimulus. The antibodies on the beads immobilized in the channel were shown to bind digoxin and a competitor fluorescent ligand from a flow stream in a quantitative competitive assay format that reported the digoxin concentration. The antibodies could be replenished for each immunoassay trial, using the reversible, temperature-controlled immobilization process. This technique allows reagent immobilization immediately prior to an analytical procedure, following the removal of previously utilized beads, guaranteeing fresh and active immobilized biomolecules. Furthermore, it provides a simple approach to multiplexing through the simultaneous or sequential injection of different antibody-coated bead species, potentially at multiple sites in the integrated device channels.

Introduction

Many important bioanalytical techniques require an immobilized, biochemically active phase. Such techniques include affinity chromatography, microtiter plate-based immunoassays, genomic and proteomic microarray analysis,[1,2] and micro/nanobead-based assays and separation processes. The translation of equivalent strategies to the microfluidic environment has relied on three broad categories of biomolecular immobilization techniques: surface modification of microfluidic channel walls,[3-8] packing of microfluidic channels with biomolecule-bearing beads,[9-14] and packing of microfluidic channels with biomolecule-bearing porous slabs.[15,16]

A disadvantage which most current microfluidic immobilization systems share is their inherent irreversibility. Once a channel is packed with beads or a monolithic polymer, or a channel surface has been chemically modified, there is no simple way for the device end user to remove or renew the immobilized molecule, or to add a new immobilized molecule. This limits the flexibility of device manufacturing, since each device must be manufactured with a specific immobilized biochemistry for a specific application. It also limits device lifetime, both on the shelf and in use, since biomolecules are often fragile, and non-renewable immobilized molecules will eventually lose activity.

Several researchers have demonstrated heterogeneous microfluidic immunoassays based on immobilized antibodies.[3,6,12] Microfluidic bioanalytical assays that operate without an immobilized phase have also been demonstrated. Such approaches include an assay based on the rate of diffusion of antibody-antigen complexes in solution[17,18] and a technique for maintaining beads in place in a recirculating flow stream without permanently immobilizing them.[19]

The work presented here demonstrates the application of a reversible bead immobilization technique which we have recently described[20] for the immobilization of immunoassay reagents within a microfluidic channel in an on-demand, spatially and temporally controlled, and reversible fashion. The digoxin antibody–antigen couple was used as a model competitive immunoassay system[21-24] to show how temperature-responsive bioanalytical beads can be utilized to couple the capture and release of target analytes for quantitative analysis.

Experimental

Materials

Digoxin and the biotinylated monoclonal murine anti-digoxin IgG (clone DI-22) were obtained from Sigma (St. Louis, MO). BODIPY® FL digoxigenin was obtained from Molecular Probes (Eugene, OR). Wild-type streptavidin was expressed and purified according to a previously published protocol.[25] The *N*-hydroxysuccinimidyl ester of poly(*N*-isopropylacrylamide) (NHS-PNIPAAm) was synthesized according to a previously published protocol.[26] 100 nm diameter Polybead® Amino Microspheres from Polysciences (Warrington, PA) were co-modified with PNIPAAm and 3.4 kDa poly(ethylene glycol)–biotin (PEG-b) (Shearwater Corporation, Huntsville, AL) as previously described.[20] PET sheets used in the fabrication of the microfluidic device were obtained from Fralock, Inc. (San Carlos, CA).

Preparation of antibody-coated beads

The antibody-bearing beads used in this experiment are described schematically in Fig. 1a. PNIPAAm and PEG-b doubly modified beads were incubated 15 minutes with equimolar (relative to immobilized biotin groups) quantities of streptavidin in pH 7.6 phosphate buffered saline (PBS, 50 mM phosphate, 5 mM NaCl). To remove any unbound streptavidin, the beads were centrifuged at 16 600*g* for 15 minutes at 4 °C. The supernatant was removed and the beads were resuspended in pH 7.6 PBS. This suspension was vortexed and agitated at 4 °C for 2 hours to assure that no bead aggregates remained. Biotinylated anti-digoxin IgG was then loaded onto the beads by adding it to the streptavidin-coated bead suspension at a 20-fold molar excess of streptavidin (assuming streptavidin tetramers bound at a 1 : 1 stoichiometry to biotin moieties in the first step).

DOI: 10.1039/b315394k

The bead suspension injected into the microfluidic channel consisted of 0.10 wt% doubly modified b-PEG/PNIPAAm beads loaded with streptavidin and anti-digoxin IgG, 0.40 wt% singly modified PNIPAAm beads, and 2.5 mg mL^{-1} free PNIPAAm in pH 7.6 PBS. The singly modified PNIPAAm beads and free PNIPAAm were added to decrease the concentration of doubly modified beads required to form a continuous adherent network on the channel walls, and to thereby conserve protein reagents. The suspension was degassed by agitation under vacuum for approximately five minutes immediately prior to use.

Microfluidic device

Experiments took place in what was described in our previous publication as a "type A" channel.[20] Briefly, the device was constructed from stacked layers of laser-machined PET. It consisted of a primary channel with one input port and one output port, with dimensions of 54 mm × 4 mm (at the widest point in the channel) × 300 μm. A small injection channel for introducing smart bead suspension led into the primary channel. Temperature control was accomplished *via* incorporation of a thin-film Therma-Clear™ heater and a HeaterStat™ electronic feedback controller (both from Minco, Minneapolis, MN). When the heater was activated, the controller maintained the temperature in a 20 mm-long region of the channel between 33 and 37 °C (this range of temperatures reflects the precision of the controller). In experiments, the heater was activated to trigger the bead aggregation caused by hydrophilic-to-hydrophobic PNIPAAm phase transition and later deactivated to reverse that process.

The assembled device was mounted in a microfluidic manifold incorporating an aluminium pressure plate and polydimethylsiloxane (PDMS) gaskets to seal the input and output ports of the device to polyether ether ketone (PEEK) tubing. Computer-controlled syringe pumps (Kloehn Co., Ltd., Las Vegas, NV) were used to drive the flow through the devices, as described in our previous publication.[20]

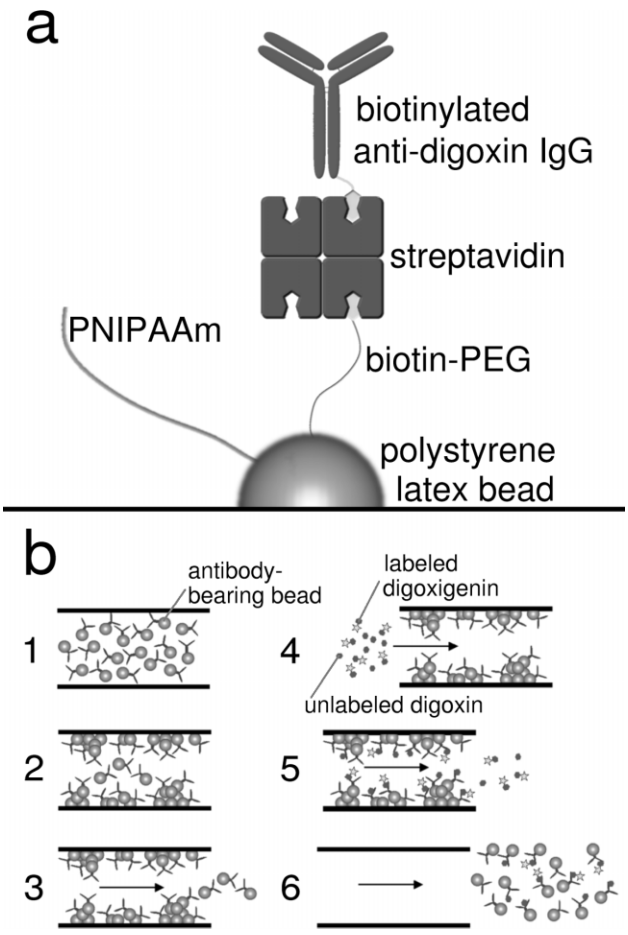

Fig. 1 Diagrammatic representations of the smart bead immunoassay system. a: The assembled smart bead construct. A 100 nm diameter latex nanobead bead is surface-conjugated with biotin–PEG and PNIPAAm. Streptavidin is bound to the exposed biotin, providing a binding site for the biotinylated anti-digoxin IgG. b: A schematic of the experimental protocol. Suspended smart beads are loaded into the PET microfluidic channel (1). The temperature in the channel is then increased from room temperature to 37 °C, resulting in aggregation and adhesion of the beads to the channel wall (2). Flow is initiated (the presence and direction of flow is indicated by an arrow in this diagram), washing unadsorbed beads out of the channel (3). A mixture of fluorescently labeled digoxigenin (at a fixed concentration) and digoxin (at varying concentrations) is flowed into the channel (4); components of this mixture that fail to bind the immobilized antibodies are washed through (5). Since digoxin and labeled digoxigenin compete for antibody binding, the higher the concentration of digoxin, the greater the amount of labeled digoxigenin that will flow through at this step. Finally, the temperature in the channel is reduced, and the aggregation–absorption process reversed as antigen-bound beads leave the channel with the flow stream (6).

Digoxin immunoassay

The immunoassay protocol is described schematically in Fig. 1b. Two hundred microlitres of the mixed bead suspension were injected *via* the bead injection channel, connected by the manifold to a short length of PEEK tubing. After bead injection, this tubing was closed off with a standard HPLC tubing valve, preventing flow through the injection channel. The input port of the primary channel was connected to the output of a flow injection valve that allowed the operator to select between two flow sources: a 0.3 mL sample loop and a 1.5 mL sample loop. The 1.5 mL sample loop was filled with degassed PBS. The 0.3 mL sample loop contained BODIPY® FL digoxigenin in degassed PBS at a concentration of 2.5 μM mixed with digoxin at a concentration of 0, 1.28, 2.56, or 12.8 μM. The heater was activated in the absence of flow for 10 minutes. The pumps were then activated, pushing buffer from the 1.5 mL sample loop through the system at a rate of 20 μL min^{-1}. Fluid flowing through the device was captured at the exit of the manifold output tubing in 50 μL aliquots. After 2.5 minutes of buffer wash, the injection valve was switched to the 0.3 mL sample loop, allowing the labeled digoxigenin/digoxin sample to flow into the device. The valve was switched back to the buffer-containing sample loop after 1.25 minutes, making the volume of the digoxigenin/digoxin sample 25 μL. After allowing the sample to bind and flow-through to be washed out (27.5 minutes after the initiation of flow), the heater was deactivated while the flow was maintained at a constant rate. Aliquots were collected for an additional 15 minutes as the aggregated beads dissolved. The output aliquots were then diluted to 500 μL in deionized water and the fluorescence of each sample was measured on a Perkin Elmer LS50B fluorescence spectrophotometer (Perkin Elmer Instruments, Inc., Shelton, CT), with excitation of the BODIPY fluorophore at 492 nm and emission at 511 nm. Experiments were performed in triplicate for each concentration investigated.

The presence of beads in the output samples introduced a scattering signal in the fluorescence measurements. This signal made the measured fluorescence higher than it would be in a sample containing no beads. To correct for this effect, a set of samples containing a range of bead concentrations (determined by the OD_{600} of the samples) but no fluorescent species were analyzed in the fluorescence spectrophotometer. This analysis yielded a linear relationship between bead concentration and scattered fluorescent signal. For each immunoassay sample, the OD_{600} was measured and this linear relationship was used to determine what scattering signal to subtract from the measured fluorescence signal.

Results and discussion

The bioanalytical system described in this study utilizes the temperature-responsive polymer poly(*N*-isopropylacrylamide) (PNIPAAm) to control the aggregation and "stickiness" of biofunctionalized beads. PNIPAAm is a "smart" polymer that

undergoes a hydrophilic–hydrophobic phase transition at temperatures above the lower critical solution temperature of approximately 28 °C in aqueous buffer.[27] The phase transition is accompanied by aggregation and precipitation of PNIPAAm molecules. Several authors have reviewed the application of this property to the fields of biotechnology and biomedicine.[28-31]

We have previously shown that when PNIPAAm-coated latex beads are also modified with a biotin–PEG moiety, they can be used to form a temperature-sensitive microfluidic chromatographic resin capable of separating the biotin-binding protein streptavidin from a flow stream.[20] This system has been further developed here to demonstrate its capacity to provide the key elements of an in-channel immunoassay.

The injectable immunoassay system is described schematically in Fig. 1. Fig. 1a is a diagram of the antibody-bearing beads. The 100 nm amine-coated polystyrene latex beads were modified using NHS-ester chemistry with two separate species: 11 kDa PNIPAAm and 3.4 kDa biotin-PEG. Approximately 40% of the amine groups on each bead (*ca.* 20 000 per bead) were biotinylated, as measured by the 2-(4′-hydroxyazobenzene) benzoic acid (HABA) assay.[32] Streptavidin was then complexed to the beads, followed by complexation of the biotinylated anti-digoxin IgG to the free streptavidin binding sites.

The digoxin/digoxigenin antigen system was used as a model for demonstrating the key steps of a competitive immunoassay. A schematic of the model protocol is provided in Fig. 1b. The stimuli-responsive beads displaying the anti-digoxin antibody (step 1) were heated above the LCST of the grafted PNIPAAm to immobilize the aggregated bead network on the channel surface in the heated region (step 2). Channel temperature control was accomplished using a system that maintained the channel temperature between 33 and 37 °C when activated, as determined by placing a thermocouple in the channel under no-flow conditions. Though the temperature cannot be expected to be uniform throughout the channel, PNIPAAm phase transition occurs over a very narrow temperature range, and the polymer can be expected to be in its hydrophobic phase so long as the local temperature is above ~28 °C under these buffer conditions. Following heating and wash through of unbound beads (step 3), a sample containing both the target antigen molecule (digoxin) and a fluorescently labeled antigen analog (BODIPY® FL digoxigenin) was flowed through the channel (steps 4 and 5). A constant concentration of the labeled digoxigenin was used in all experiments. Since the two species in the sample compete for antibody binding, the amount of labeled digoxigenin that binds depends on the concentration of target digoxin in the sample. The concentration of digoxin in a given sample can therefore be determined by tracking the amount of antibody-bound fluorescent digoxigenin. After the sample had been allowed to flow through the channel, the heater was deactivated, lowering the channel temperature below the PNIPAAm LCST and causing the beads to disaggregate and leave with the flow stream (step 6). Any antibody-bound digoxin or digoxigenin molecules left the channel with these beads. Throughout this procedure, 50 μL aliquots were collected at the channel output for subsequent fluorescence analysis.

The successful competitive capture of digoxin and digoxigenin is shown in Fig. 2. The fluorescent intensities of the system output fractions are given as fractions of total fluorescence measured over the course of the experiment. The zero point on the *x*-axis corresponds to the initiation of pump-driven flow, after bead aggregation and adhesion had been allowed to take place in the heated channel. The initially elevated fluorescence values at the 50 and 100 μL points are due to non-adherent beads being washed out of the channel. Previous work has shown that approximately 50% of the thermally immobilized bead suspension adheres to the channel walls under flow conditions.[20] Given the ratio of antibody loading on the beads, this implies that approximately 600 picomoles of antibody are available on the channel surfaces for binding to digoxin/digoxigenin. This is approximately a ten-fold excess relative to the total amount of labeled digoxigenin injected. The peaks that begin at 250 μL represent unbound BODIPY® FL digoxigenin flowing past the immobilized antibodies and out of the channel. At the 550 μL point, the heater was deactivated, lowering the temperature in the channel and resulting in the dissolution of the adherent bead matrix. The beads were washed out of the channel, along with the bound fractions of digoxin and BODIPY® FL digoxigenin. Previous work has shown the process of bead release upon decrease in channel temperature to be near 100% efficient.[20] The fluorescence signal from the bound digoxigenin is observed as the peak beginning at the 600 μL point. As digoxin concentration increases, the flowthrough peak at 250 μL becomes larger while the elution peak at 600 μL becomes correspondingly smaller. This change is due to digoxin competition with fluorescent digoxigenin for binding to the immobilized antibodies. As less labeled digoxigenin binds the beads, more passes through the channel with the flowthrough peak (labeled A on Fig. 2), and less flows out with the beads in the elution peak (B).

The errors at each individual point in Fig. 2 make it difficult to distinguish between digoxin concentrations. However, by considering total peak area, varying digoxin concentrations can be easily discriminated, as shown in Fig. 3. The plot in Fig. 3a corresponds to the flowthrough peak, while Fig. 3b corresponds to the elution peak. Peak areas were obtained by simply integrating the peaks shown in Fig. 2, after drawing straight lines between the data points. The flowthrough peak was integrated from the 200 μL point to the 450 μL point, while the elution peak was integrated from the 550 μL point to the 700 μL point. While the 1.28 and 2.56 μM points remain statistically indistinguishable in both plots, the 0 and 12.8 μM points are distinguishable from all other points.

In this model device format, concentrations of digoxin as low as 1.28 μM could be reliably determined and varying concentrations of digoxin ranging over an order of magnitude could be distinguished. The flowthrough peak data were sufficient to provide the full calibration curve throughout this digoxin concentration range. These results demonstrate that this system is capable of reporting the competitive binding and measurement of a target antigen in a

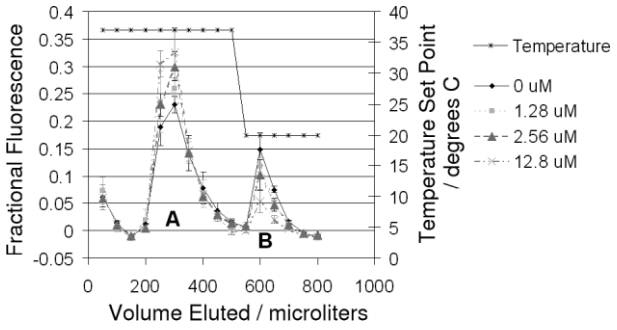

Fig. 2 The fluorescence intensity of the device output throughout the digoxin immunoassay experiments is shown. The *x*-axis corresponds to the total volume of fluid that has flowed through the device with each point representing a 50 μL sample. The left *y*-axis corresponds to the fluorescence intensity measured in each of the samples, normalized to the total fluorescence observed throughout the duration of the experiment. The right *y*-axis corresponds to the set-point temperature on the heating control unit. Four of the data traces are for fluorescence data. These are the traces corresponding to immunoassays with varying concentrations of digoxin: 0 μM (diamonds), 1.28 μM (squares), 2.56 μM (triangles), and 12.8 μM (X-marks). The fifth data trace (asterisks) represents the temperature. The temperature set point was maintained at 37 °C until the 550 μL point, at which point it was decreased to 20 °C. In each of the fluorescence data traces, two peaks were observed. The first peak (A, the flowthrough peak), beginning at the 250 μL point, corresponds to unbound labeled digoxigenin in solution flowing past the antibodies on the immobilized beads. At higher digoxin concentrations, less digoxigenin can bind to the antibodies, and the size of this peak increases. The second peak (B, the elution peak), beginning at the 600 μL point, corresponds to the labeled digoxigenin bound to the antibody-coated beads eluting from the channel walls. At higher digoxin concentrations, less digoxigenin is bound to the beads, and the size of this peak decreases. Error bars are ± one standard deviation over three experiments.

format that can conveniently provide a wide range of concentration dependences.

Because the fluorescence measurements were made on arbitrary flow-through aliquots (related to the channel dimensions and volumes) that were subsequently diluted to accommodate measurements in a standard benchtop fluorometer, the particular accessible range of digoxin concentrations reported in this study does not represent the intrinsic sensitivity of this system. That sensitivity will ultimately be a function of the device and detection design, and on-chip detection schemes and optical probes that minimize dilution and maximize signal should provide particularly important sensitivity enhancements. Finally, it is important to note that since the process of bead adhesion to the channel wall is not stoichiometric, the amount of immobilized antibody is expected to vary slightly with each trial. This imprecision results in the relatively large error bars seen in Fig. 2. However, the data presented in Fig. 3 demonstrate that meaningful results can be extracted from this platform even in light of the variations in amount of antibody immobilized.

Conclusions

The reversible biomolecular immobilization facilitated by this technique allowed for all experiments to be performed in a single device over a period of several weeks with a fresh immobilized antibody substrate for each new experiment. Loading this substrate took only ten minutes, and it was not necessary to remove the device from the fluidic manifold connecting it to the sample delivery system. This platform is completely general in that any molecule that can be biotinylated or otherwise bound to the surface of a latex bead (*e.g.* enzymes, ligands, oligonucleotides) can be immobilized in microfluidic channels *via* this technology. Finally, the precise and reversible temperature-responsive nature of the smart polymer gives engineers a novel means of control for microfluidic processes, since the spatial distribution of immobilized molecules in a microfluidic device can be controlled merely by controlling the temperature at various locations in the device.

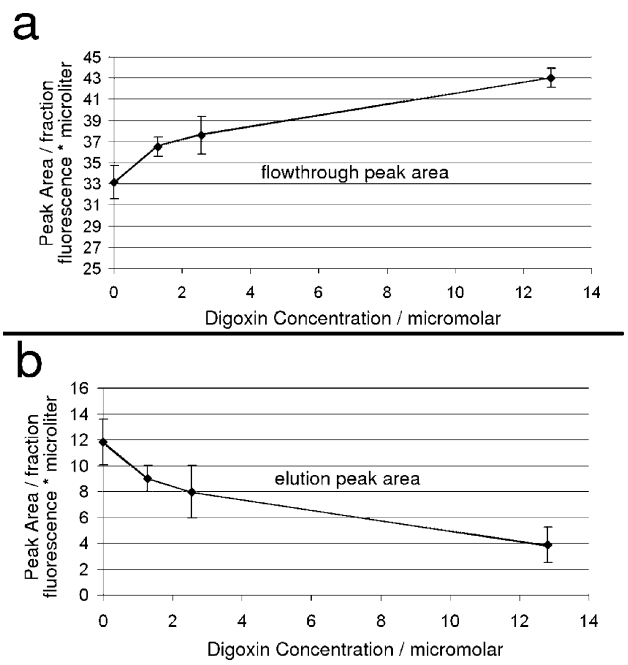

Fig. 3 Integrated flowthrough (a) and elution (b) peak areas are shown as a function of digoxin concentration. a: Integrated area of the flowthrough (A) peaks from Fig. 2 as a function of digoxin concentration. As digoxin concentration increases, so does competition for antibody binding, and the amount of labeled digoxigenin bound to the immobilized antibodies decreases. The amount of digoxigenin flowing directly through the system therefore increases, increasing the size of this peak. b: Integrated area of the elution (B) peaks as a function of digoxin concentration. Increasing concentrations of digoxin decrease the amount of labeled digoxigenin bound to the eluting beads, thereby decreasing the size of this peak. All error bars are ± one standard deviation over three experiments.

Acknowledgements

The authors would like to express their gratitude to the NIH for funding (Grant EB000252).

References

1 P. Cutler, *Proteomics*, 2003, **3**, 3–18.
2 M. F. Templin, D. Stoll, M. Schrenk, P. C. Traub, C. F. Vohringer and T. O. Joos, *Trends Biotechnol.*, 2002, **20**, 160–166.
3 A. Dodge, K. Fluri, E. Verpoorte and N. F. de Rooij, *Anal. Chem.*, 2001, **73**, 3400–3409.
4 A. Schwarz, J. S. Rossier, E. Roulet, N. Mermod, M. A. Roberts and H. H. Girault, *Langmuir*, 1998, **14**, 5526–5531.
5 A. Papra, A. Bernard, D. Juncker, N. B. Larsen, B. Michel and E. Delamarche, *Langmuir*, 2001, **17**, 4090–4095.
6 T. L. Yang, S. Y. Jung, H. B. Mao and P. S. Cremer, *Anal. Chem.*, 2001, **73**, 165–169.
7 H. B. Mao, T. L. Yang and P. S. Cremer, *Anal. Chem.*, 2002, **74**, 379–385.
8 L. M. Shamansky, C. B. Davis, J. K. Stuart and W. G. Kuhr, *Talanta*, 2001, **55**, 909–918.
9 H. Andersson, W. van der Wijngaart, P. Enoksson and G. Stemme, *Sens. Actuators B*, 2000, **67**, 203–208.
10 T. Buranda, J. Huang, V. H. Perez-Luna, B. Schreyer, L. A. Sklar and G. P. Lopez, *Anal. Chem.*, 2002, **74**, 1149–1156.
11 S. Ekstrom, J. Malmstrom, L. Wallman, M. Lofgren, J. Nilsson, T. Laurell and G. Marko-Varga, *Proteomics*, 2002, **2**, 413–421.
12 K. Sato, M. Tokeshi, T. Odake, H. Kimura, T. Ooi, M. Nakao and T. Kitamori, *Anal. Chem.*, 2000, **72**, 1144–1147.
13 T. Richter, L. L. Shultz-Lockyear, R. D. Oleschuk, U. Bilitewski and D. J. Harrison, *Sens. Actuators B*, 2002, **81**, 369–376.
14 L. Ceriotti, N. F. de Rooij and E. Verpoorte, *Anal. Chem.*, 2002, **74**, 639–647.
15 C. Ericson, J. Holm, T. Ericson and S. Hjerten, *Anal. Chem.*, 2000, **72**, 81–87.
16 D. S. Peterson, T. Rohr, F. Svec and J. M. J. Fréchet, *Anal. Chem.*, 2002, **74**, 4081–4088.
17 A. Hatch, A. E. Kamholz, K. R. Hawkins, M. S. Munson, E. A. Schilling, B. H. Weigl and P. Yager, *Nat. Biotechnol.*, 2001, **19**, 461–465.
18 A. E. Kamholz, B. H. Weigl, B. A. Finlayson and P. Yager, *Anal. Chem.*, 1999, **71**, 5340–5347.
19 G. L. Lettieri, A. Dodge, G. Boer, N. F. de Rooij and E. Verpoorte, *Lab Chip*, 2003, **3**, 34–39.
20 N. Malmstadt, P. Yager, A. S. Hoffman and P. S. Stayton, *Anal. Chem.*, 2003, **75**, 2943–2949.
21 S. A. Jortani and R. Valdes, *Crit. Rev. Clin. Lab. Sci.*, 1997, **34**, 225–274.
22 F. T. Hafner, R. A. Kautz, B. L. Iverson, R. C. Tim and B. L. Karger, *Anal. Chem.*, 2000, **72**, 5779–5786.
23 F. Szurdoki, K. L. Michael and D. R. Walt, *Anal. Biochem.*, 2001, **291**, 219–228.
24 Y. N. Shim and I. R. Paeng, *Bull. Korean Chem. Soc.*, 2003, **24**, 70–74.
25 A. Chilkoti, P. H. Tan and P. S. Stayton, *Proc. Natl. Acad. Sci. USA*, 1995, **92**, 1754–1758.
26 Z. L. Ding, G. H. Chen and A. S. Hoffman, *Bioconjugate Chem.*, 1996, **7**, 121–125.
27 M. Heskins and J. E. Guillet, *J. Macromol. Sci.-Chem.*, 1968, **A2**, 1441–1455.
28 A. S. Hoffman, *J. Controlled Release*, 1987, **6**, 297–305.
29 A. S. Hoffman, P. S. Stayton, V. Bulmus, G. H. Chen, J. P. Chen, C. Cheung, A. Chilkoti, Z. L. Ding, L. C. Dong, R. Fong, C. A. Lackey, C. J. Long, M. Miura, J. E. Morris, N. Murthy, Y. Nabeshima, T. G. Park, O. W. Press, T. Shimoboji, S. Shoemaker, H. J. Yang, N. Monji, R. C. Nowinski, C. A. Cole, J. H. Priest, J. M. Harris, K. Nakamae, T. Nishino and T. Miyata, *J. Biomed. Mater. Res.*, 2000, **52**, 577–586.
30 I. Y. Galaev and B. Mattiasson, *Trends Biotechnol.*, 1999, **17**, 335–340.
31 H. G. Schild, *Prog. Polym. Sci.*, 1992, **17**, 163–249.
32 N. M. Green, *Methods Enzymol.*, 1970, 418.